

Autocrine loops with positive feedback enable context-dependent cell signaling

S. Y. SHVARTSMAN,¹ M. P. HAGAN,² A. YACOUB,² P. DENT,²
H. S. WILEY,³ AND D. A. LAUFFENBURGER⁴

¹*Department of Chemical Engineering and Lewis Sigler Institute for Integrative Genomics, Princeton University, Princeton, New Jersey 08544;* ²*Radiation Oncology, Virginia Commonwealth University/Medical College of Virginia, Richmond, Virginia 23298-0058;* ³*Fundamental Sciences Division, Pacific Northwest National Laboratory, Richland, Washington 99352;* and ⁴*Division of Bioengineering and Environmental Health, Department of Chemical Engineering, and Center for Cancer Research, Massachusetts Institute of Technology, Cambridge, Massachusetts 02139*

Received 11 June 2001; accepted in final form 15 October 2001

Shvartsman, S. Y., M. P. Hagan, A. Yacoub, P. Dent, H. S. Wiley, and D. A. Lauffenburger. Autocrine loops with positive feedback enable context-dependent cell signaling. *Am J Physiol Cell Physiol* 282: C545–C559, 2002. First published October 17, 2001; 10.1152/ajpcell.00260.2001.—We describe a mechanism for context-dependent cell signaling mediated by autocrine loops with positive feedback. We demonstrate that the composition of the extracellular medium can critically influence the intracellular signaling dynamics induced by extracellular stimuli. Specifically, in the epidermal growth factor receptor (EGFR) system, amplitude and duration of mitogen-activated protein kinase (MAPK) activation are modulated by the positive-feedback loop formed by the EGFR, the Ras-MAPK signaling pathway, and a ligand-releasing protease. The signaling response to a transient input is short-lived when most of the released ligand is lost to the cellular microenvironment by diffusion and/or interaction with an extracellular ligand-binding component. In contrast, the response is prolonged or persistent in a cell that is efficient in recapturing the endogenous ligand. To study functional capabilities of autocrine loops, we have developed a mathematical model that accounts for ligand release, transport, binding, and intracellular signaling. We find that context-dependent signaling arises as a result of dynamic interaction between the parts of an autocrine loop. Using the model, we can directly interpret experimental observations on context-dependent responses of autocrine cells to ionizing radiation. In human carcinoma cells, MAPK signaling patterns induced by a short pulse of ionizing radiation can be transient or sustained, depending on cell type and composition of the extracellular medium. On the basis of our model, we propose that autocrine loops in this, and potentially other, growth factor and cytokine systems may serve as modules for context-dependent cell signaling.

mathematical model; epidermal growth factor receptor; ligand shedding; ionizing radiation; mitogen-activated protein kinase; cross-activation

WHAT MECHANISMS ENABLE context-dependent cell signaling? That is, how can molecular interactions in the cell's microenvironment combine with those within the

cell to modulate response to a particular stimulus? In part, the specificity of a cell's response is built into the molecular makeup of signal transduction networks (37). Receptor binding by soluble ligands, such as growth factors, is translated into cellular responses by signaling pathways, which rely for their activation on a number of adaptors and enzymes. In this way, activation of identical receptors in two cells with different sets of adaptors and enzymes stimulates different signaling pathways, resulting in two different responses. The induced responses may differ in the nature of the stimulated signaling pathways and/or in the dynamic properties of their activation (48). The extracellular context, e.g., composition of the extracellular matrix (ECM), can affect the signaling response by creating the intracellular background that dynamically interacts with signaling induced by exogenous signals, such as soluble growth factors (31, 56). Previously proposed mechanisms of context-dependent "processing" of external stimuli focus on this kind of intracellular synergy of multiple inputs (63, 66). We suggest the existence of a complementary mechanism that enables cells to process external stimuli both intra- and extracellularly. This mechanism may be operative in autocrine loops formed by growth factors and their receptors.

Autocrine loops are established when soluble factors secreted by cells bind to and stimulate receptors on their own surfaces (64). Commonly, secretion of autocrine ligands is tightly regulated. In the epidermal growth factor (EGF) receptor (EGFR) system, ligands such as transforming growth factor- α (TGF- α) are synthesized in the form of membrane-bound precursors (49). Thereafter, ligand-releasing proteases, also known as "shedases" [e.g., tumor necrosis factor- α (TNF- α)-converting enzyme (TACE)], process the membrane-associated precursors into their active soluble forms

Address for reprint requests and other correspondence: D. A. Lauffenburger, Dept. of Chemical Engineering, MIT, Cambridge, MA 02139 (E-mail: lauffen@mit.edu).

The costs of publication of this article were defrayed in part by the payment of page charges. The article must therefore be hereby marked "advertisement" in accordance with 18 U.S.C. Section 1734 solely to indicate this fact.

(49, 54, 70). The characteristically high levels of cognate receptors expressed by autocrine cells make them very efficient in recapturing endogenous ligands (15, 19, 44, 53, 62, 72). Along with the mechanisms for ligand release and capture, autocrine systems are equipped with numerous mechanisms for cross activation (10, 50, 55, 75). Response to a primary stimulus, such as an exogenous growth factor, a component of the ECM, or ionizing radiation, can lead to ligand release and recapture and stimulation of intracellular signaling (16, 30, 58). In nonautocrine cells, soluble growth factors were shown to activate sheddases through the Ras-mitogen-activated protein kinase (MAPK) pathway (23, 26), one of the central pathways activated by receptor tyrosine kinases such as EGFR. This suggests that, in an autocrine EGFR system, a ligand, the receptor, the sheddase, and the intracellular signaling network can form a positive-feedback loop (52).

The spatially restricted and recurrent nature of autocrine loops makes their experimental analysis very challenging. As an aid to the experimental studies of autocrine loops in the EGFR system, we integrate the biochemical and biophysical knowledge about EGFR signaling into a mechanistic mathematical model. The model accounts for the dynamic interaction between ligand release, diffusion in the extracellular medium, receptor binding, and Ras-MAPK pathway activation. We find that the positive feedback endows autocrine cells with nontrivial signal-processing capabilities. We propose a mechanism for modulating the amplitude and duration of Ras-MAPK activation induced by external stimuli; these characteristics of MAPK signaling are critical for a number of cellular responses (48, 56). Using our model, we demonstrate that this mechanism provides a substrate for context-dependent cell signaling. Furthermore, our analysis enables the direct interpretation of the context-dependent radiation responses of autocrine cells. In human carcinoma cells, the EGFR-TGF- α autocrine loop defines cellular response to radiation (survival or death) by regulating the duration and amplitude of the Ras-MAPK activation (16).

This report is organized as follows. In COMPUTATIONAL MODEL FOR AUTOCRINE CELL-SIGNALING LOOP, we describe the modules for ligand release, binding and transport, and intracellular signaling. Then we describe how these individual modules are integrated in a model of an autocrine loop. In RESULTS, we focus exclusively on the processes defining the operation of autocrine systems. Equations and details of their analysis can be found in APPENDIX A. After identifying the key parameters governing the operation of individual modules, we proceed to analysis of the integrated system; we focus on the effects of the feedback loop formed by the receptor, the signaling cascade, and the system for ligand release. This sets up the framework for the analysis of the experiments reporting context-dependent radiation responses of autocrine cells in the DISCUSSION. These experiments support our modeling predictions, demonstrating that the composition of the extracellular medium, in this particular case the presence or

absence of ligand-binding antibodies, can critically influence the cell response.

COMPUTATIONAL MODEL FOR AUTOCRINE CELL-SIGNALING LOOP

The biochemical events that we aim to model are summarized in Fig. 1A. Initial activation of a growth factor receptor stimulates downstream signaling pathways (e.g., the Ras-MAPK pathway) that, by unknown mechanisms (23, 26), increase the activity of sheddases and lead to release of soluble growth factor(s). Localized capture of endogenous ligands increases the number of occupied receptors and initiates a secondary stimulation of the receptor and downstream signaling pathways. The positive-feedback loop—receptor/signaling/sheddase/ligand/receptor—governs the duration and amplitude of the signaling transient in response to external perturbation.

Model of Ligand Binding and Transport

Equilibrium and kinetic parameters for binding and trafficking in growth factor receptor systems, including the ErbB1–4 system, have been well documented (18, 43, 60); furthermore, experiments reporting diffusivities of growth factors in tissues have recently started to appear (21). Our model of binding and transport (Fig. 2A) accounts for the concentration of endogenous ligand (L) and the surface densities of free and occupied surface receptors (R_s and C_s , respectively). We consider a single autocrine cell; the cell is modeled as a hemisphere with radius r_{cell} , placed on an infinite plane (this mimics an autocrine cell attached to a substrate). Ligand secretion, at rate Q , is uniformly distributed over the cell surface area (A). Ligand released in the extracellular medium diffuses with constant diffusivity (D) and reversibly binds to cell surface receptors with binding constant K_d . Newly synthesized receptors arrive at the cell surface with rate S ; they are constitu-

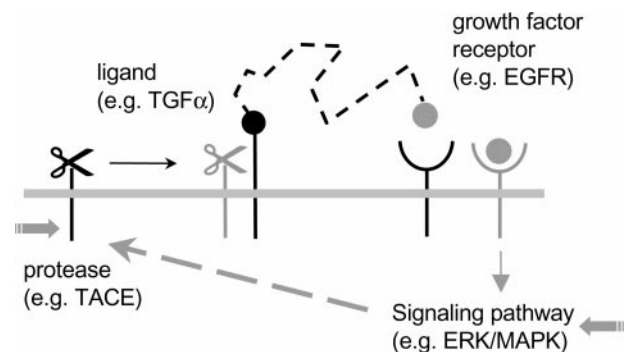


Fig. 1. Schematic illustration of ligand-induced autocrine growth factor release mediated by receptor-activated intracellular signaling. In the epidermal growth factor (EGF) receptor (EGFR) system, ligands of the EGFR are shed from the cell surface by surface metalloproteases activated (among other things) via the extracellular signal-regulated kinase (ERK)-mitogen-activated protein kinase (MAPK) cascade; the same cascade is activated when autocrine ligands bind to receptors on the surface of the releasing cell. TGF- α , transforming growth factor- α ; TACE, tumor necrosis factor- α -converting enzyme.

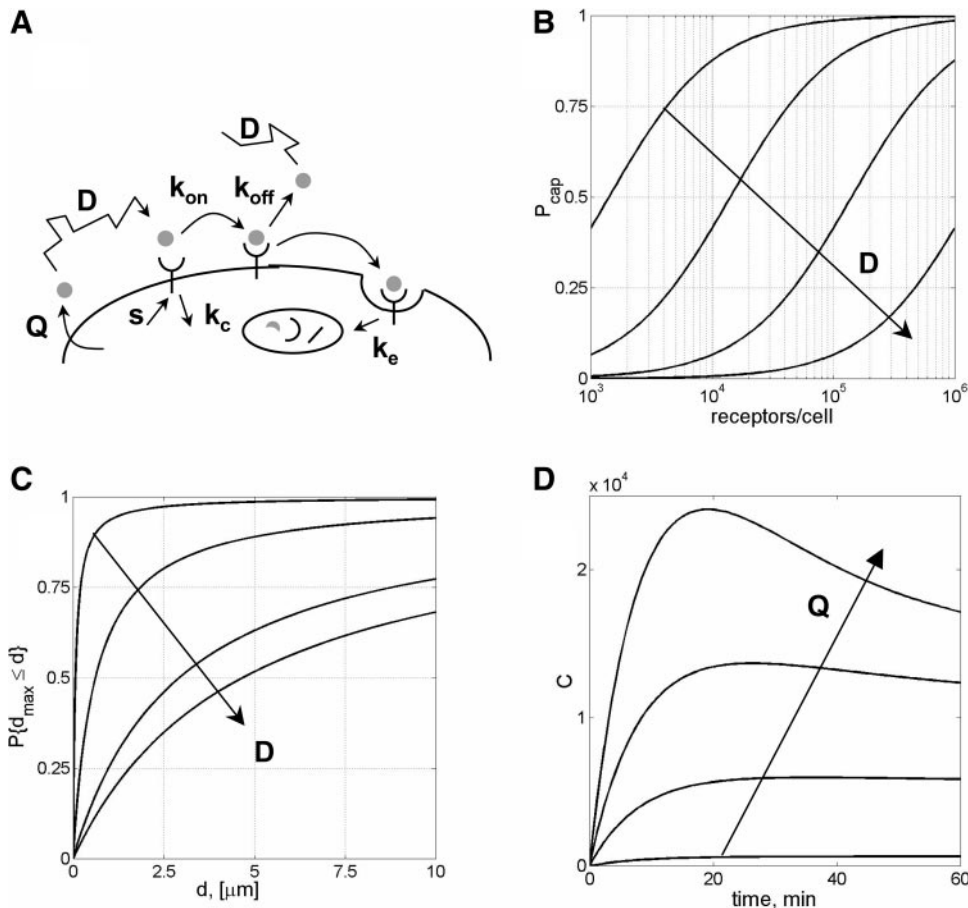


Fig. 2. *A*: model of binding and transport: ligand release, extracellular diffusion, binding to surface receptors, endocytic internalization, and reversible binding to components of the extracellular medium (see APPENDIX A for detailed description of model parameters). *B*: fraction of endogenous ligand recaptured by an autocrine cell (P_{cap}). P_{cap} is computed as a function of the total number of cell surface receptors ($R_T = S/k_e$) for several values of the extracellular ligand diffusivity (D). Values for the parameters are as follows: $k_{on} = 10^8 \text{ M}^{-1} \cdot \text{min}^{-1}$, $D = 10^{-6}, 10^{-7}, 10^{-8}, \text{ and } 10^{-9} \text{ cm}^2/\text{s}$, and cell radius (r_{cell}) = $5 \times 10^{-4} \text{ cm}$. *C*: statistical properties of the random paths followed by those endogenous ligands that have been recaptured by the cell. Cumulative distribution function of the maximal distance (d_{max}) to which a recaptured secreted ligand had diffused. Parameters are as follows: $R_T = 10^5/\text{cell}$; all other parameters as in *A*. *D*: dynamics of the number of ligand receptor complexes induced by a step change in the rate of ligand secretion from 0 to $Q \text{ mol} \cdot \text{cell}^{-1} \cdot \text{min}^{-1}$. Parameters are as follows: $R_T = 10^5/\text{cell}$, $r_{cell} = 5 \times 10^{-4} \text{ cm}$, $k_{on} = 10^8 \text{ M}^{-1} \cdot \text{min}^{-1}$, $K_d = 1 \text{ nM}$, $k_e = 0.1 \text{ min}^{-1}$, $k_c = 0.02 \text{ min}^{-1}$, and extracellular ligand diffusivity (D) = $10^{-7} \text{ cm}^2/\text{s}$. For transients, $Q = 100, 1,000, 3,000, \text{ and } 5,000 \text{ mol} \cdot \text{cell}^{-1} \cdot \text{min}^{-1}$.

tively internalized with rate constant k_c and are converted to surface complexes with rate constant k_{on} . Surface complexes dissociate with rate constant $k_{off} = k_{on}K_d$ and are removed from the cell surface by endocytosis with rate constant k_e . Endogenous ligand can reversibly bind to the extracellular “decoys” (molecules that mimic soluble antiligand antibodies) (12, 25, 44). B denotes the concentration of decoys; their interaction with ligand is characterized by the forward and reverse rate constants k_{off}^D and k_{on}^D , respectively. The extracellular concentration of ligand bound to decoys is denoted by L^B .

Model of Protease Activation

Ligand-releasing proteases have only recently been added to the “parts list” of the autocrine loops (7, 19, 54, 70); so far, mathematical modeling of protease activity has not been attempted. The main facts in the rapidly accumulating information on the molecular nature, mechanism of action, and dynamics of sheddases can be summarized as follows. Ligand-releasing proteases are not specific and are capable of processing a wide range of surface molecules (7); members of the EGFR ligand family are just one example (70). The rate of ectodomain cleavage depends on the juxtamembrane domain of the precursor molecule (20, 51). Sheddases are under the control of multiple intracellular signaling pathways;

secretion is composed of a slow process mediating the constitutive release and faster inducible process (23, 26). The inducible activation can occur as fast as 10–15 min after application of the stimulus (26). The activation of protease is followed by its removal from the surface, most likely via the endocytic pathway (17). In our model (Fig. 3A), we assume that newly synthesized protease is inserted in the membrane with the rate S_P and constitutively internalized with the rate constant k_c^P . The protease is converted to the “active” form with the rate constant k_a^P ; the active form is internalized via endocytosis with the rate constant k_e^P . The model is formulated in terms of variables P and P_a , denoting the amount of protease in the inactive and active states (see APPENDIX A).

Model of Signaling Cascade

Previously introduced dynamic models of the MAPK cascade account for the dynamic changes of enzymes at the three levels of the cascade and the negative feedback exerted by the active form of the last enzyme on the input to the network (34, 39, 47). For our purposes, we need the simplest possible model that would be consistent with the previous descriptions and evolve on the time scales observed in time-resolved assays of MAPK activity (2). Our model of the MAPK cascade (Fig. 3A) consists of three enzymes, E_1 , E_2 , and E_3 (Fig. 4A). The three stages in the cascade model the sequen-

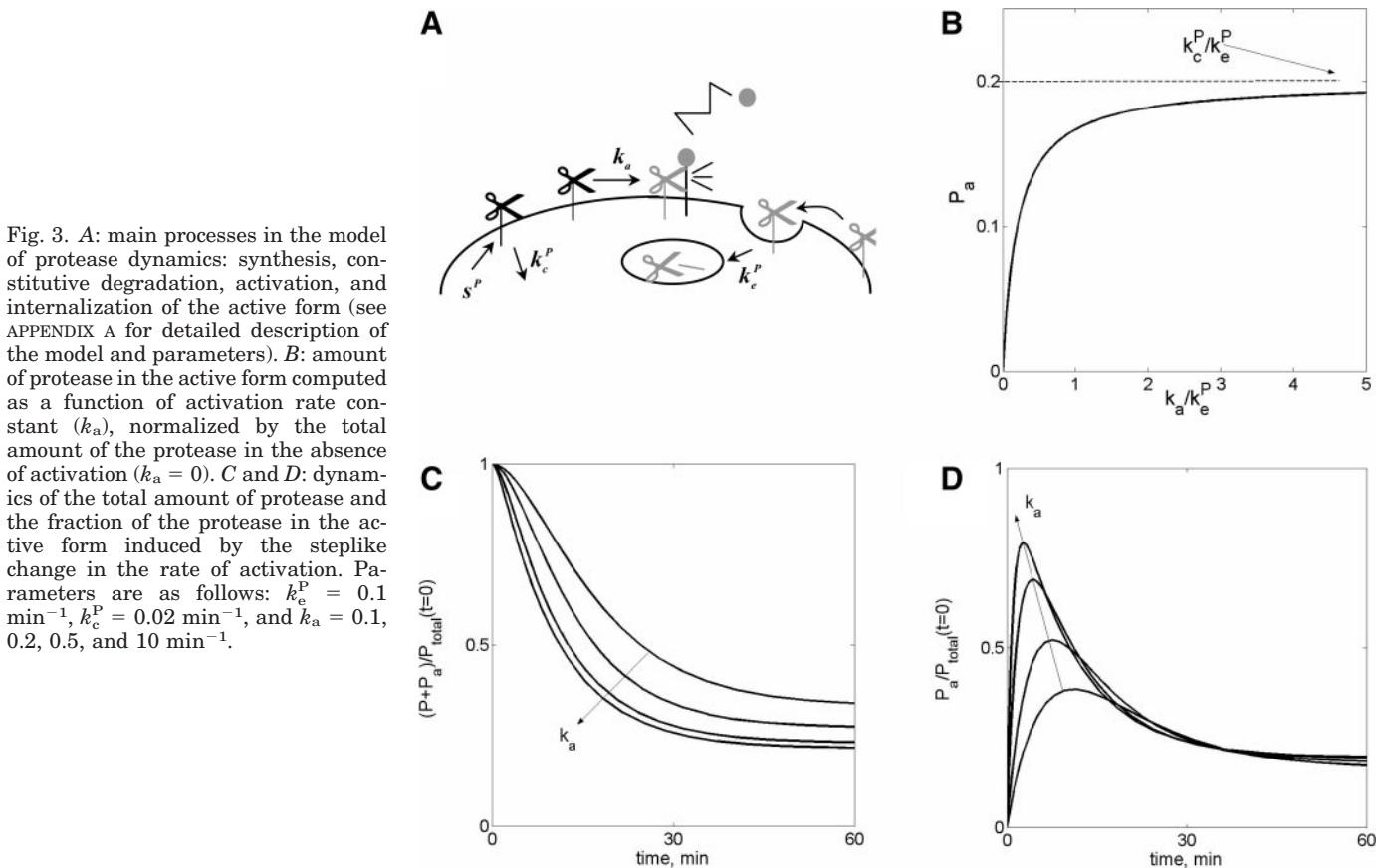


Fig. 3. *A*: main processes in the model of protease dynamics: synthesis, constitutive degradation, activation, and internalization of the active form (see APPENDIX A for detailed description of the model and parameters). *B*: amount of protease in the active form computed as a function of activation rate constant (k_a), normalized by the total amount of the protease in the absence of activation ($k_a = 0$). *C* and *D*: dynamics of the total amount of protease and the fraction of the protease in the active form induced by the steplike change in the rate of activation. Parameters are as follows: $k_c^p = 0.1 \text{ min}^{-1}$, $k_c^p = 0.02 \text{ min}^{-1}$, and $k_a = 0.1, 0.2, 0.5,$ and 10 min^{-1} .

tial activation of Raf, MAPK kinase (MEK), and MAPK (47). “Kinases” at each level of the cascade can be in one of the two forms, “base” and “active,” which are interconverted by two distinct enzymes. Active forms of E_1 and E_2 catalyze forward reactions of the following stages. In the model, the “phosphatases” catalyzing reactions 2, 4, and 6 are constitutively active. The maximal rate of reaction 1 depends on the magnitude of the input to the cascade (I). The phosphorylated form

of E_3 decreases the input to the cascade reaction; this reflects the fact that formation of the signaling complex stimulating the input to the cascade can be negatively regulated by the active form of extracellular signal-regulated kinase (ERK) type 2 (ERK2) MAPK (47). Other negative feedbacks, such as receptor-mediated endocytosis and covalent modification decreasing receptor tyrosine kinase activity (e.g., via protein kinase C), operate upstream of the MAPK cascade, further

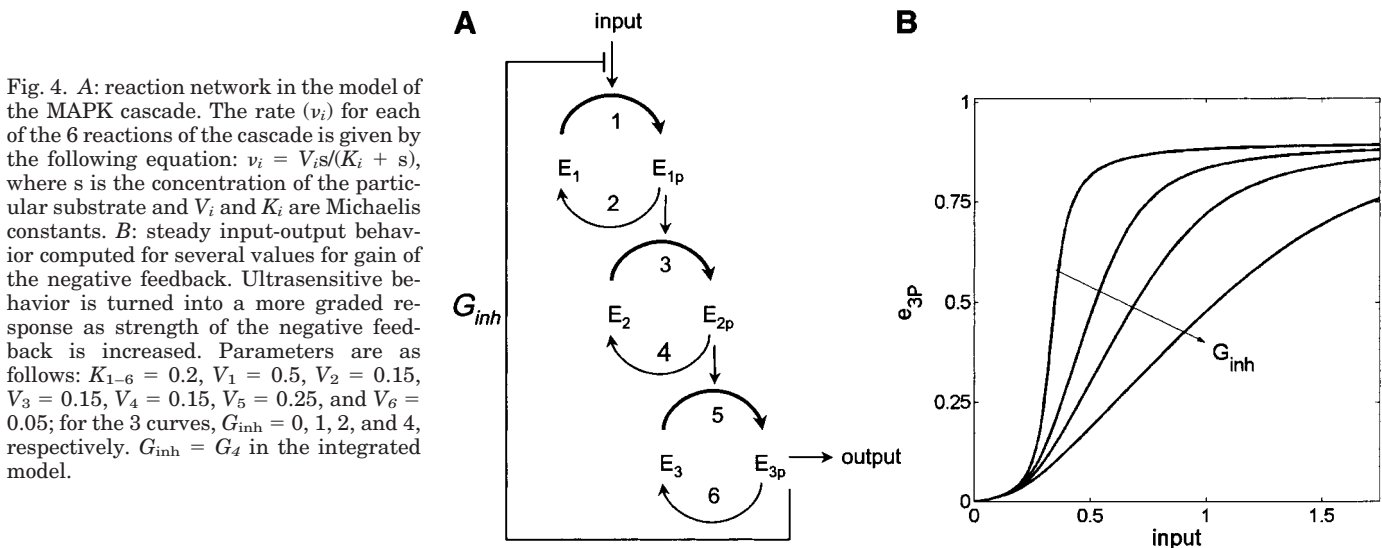


Fig. 4. *A*: reaction network in the model of the MAPK cascade. The rate (v_i) for each of the 6 reactions of the cascade is given by the following equation: $v_i = V_i s / (K_i + s)$, where s is the concentration of the particular substrate and V_i and K_i are Michaelis constants. *B*: steady input-output behavior computed for several values for gain of the negative feedback. Ultrasensitive behavior is turned into a more graded response as strength of the negative feedback is increased. Parameters are as follows: $K_{1-6} = 0.2$, $V_1 = 0.5$, $V_2 = 0.15$, $V_3 = 0.15$, $V_4 = 0.15$, $V_5 = 0.25$, and $V_6 = 0.05$; for the 3 curves, $G_{inh} = 0, 1, 2,$ and 4 , respectively. $G_{inh} = G_4$ in the integrated model.

serving to provide the network with transient inputs (36, 50, 57).

Coupled System

The integrated model is assembled from the individual blocks on the basis of the information available about their coupling (Fig. 5). Ligand-mediated receptor phosphorylation and signaling complex assembly, linking the act of ligand receptor binding to the MAPK cascade, were recently modeled by a sequence of reversible reactions (6, 8, 41) for receptor phosphorylation and signaling complex assembly; detailed kinetic modeling of these events is beyond the scope of this work. Activation of ligand-releasing proteases mediated by the MAPK has been conclusively demonstrated (23, 26, 29). The first kinetic analysis of the proteolytic release of the EGF-family ligands has been recently reported; it has been shown that the rate of ligand release obeys pseudo-first-order kinetics with respect to the amount of surface protease (20). In the absence of more detailed information, linear gains (in other words, linear proportionality of cause and effect) provide the simplest possible descriptions of the (nonlinear) interconnections between the modules comprising the autocrine loop. First, the endogenous input to the signaling cascade is proportional to the number of surface complexes. Second, the rate constant of protease activation is proportional to the amount of the active form of the last enzyme in the signaling cascade. Finally, the rate of ligand secretion is proportional to the fraction of the protease in the active form. The system of equations describing the integrated model is presented in APPENDIX A.

RESULTS

Analysis of the Model

Transport and binding. The rate of diffusion of endogenous ligand away from the cell surface is defined as the number of molecules released per unit area in unit of time; it is termed the “flux” (F). F depends on the amount of secreted ligand and the ability of the

autocrine cell to remove the endogenous ligand from the extracellular medium by binding and receptor-mediated endocytosis. The ratio of F to the rate of ligand secretion quantifies the fraction of autocrine ligands escaping from the releasing cell. The remaining fraction of secreted ligand defines the (steady) probability of ligand capture: $P_{cap} \equiv 1 - F/Q$. Within our model, P_{cap} is related to the binding/transport parameters by the following expression

$$Da = \frac{P_{cap}Au}{\gamma} + \frac{P_{cap}}{\delta(1 - P_{cap})} \tag{1}$$

where

$$Au = \frac{Qr_{cell}}{ADK_d}, \quad Da = \frac{k_{on}r_{cell}S}{k_cDA}, \quad \gamma = \frac{k_c}{k_{off}}, \quad \delta = \frac{k_e}{k_e + k_{off}} \tag{2}$$

The first of these dimensionless groups (Au) is the autocrine number, equal to the ratio of the ligand concentration at the cell surface in the absence of surface receptors to the dissociation constant of a ligand-receptor pair. The second, Da , is the Damköhler number, which quantifies the relative importance of ligand binding and transport (14). The third group, γ , compares the rate at which free receptors are removed by constitutive internalization with the rate at which they are freed by dissociating complexes. Finally, for a bound ligand, δ is the probability of being internalized. Detailed analysis of *Eq. 1* is reported elsewhere (62).

Note that when calculating the recaptured fraction of autocrine ligands using *Eq. 1*, we discount those that were bound by the cell, dissociated, and then “lost” to the extracellular medium. However, even those ligands that had been on the surface only transiently may contribute to receptor activation. By setting the rate of ligand dissociation to zero (*Eq. 1*), we consider only the processes that occur before the first binding event. In this way, we obtain a fraction of endogenous ligands that were bound by the cell at least once

$$P_{cap} = Da/(1 + Da) \tag{3}$$

This limit of *Eq. 1* is the classic expression obtained by Berg and Purcell (5, 61). High capturing efficiency is promoted by the high number of cognate receptors, fast forward binding, and low extracellular ligand diffusivity. Autocrine cells equipped with the EGFR autocrine loops often express more surface receptors (10^5 – 10^6) (19, 53) than nonautocrine-regulated cells (10^3 – 10^4 receptors), which may utilize endocrine mechanisms for their growth and survival. Furthermore, interaction of secreted growth factors with the components of the ECM has the potential to make their effective diffusivity after cleavage and release relatively low (21). We conclude that, at least in the EGFR system, autocrine cells have the potential to recover a significant fraction of endogenous ligand. Figure 2B presents the recaptured fraction of autocrine ligands computed as a function of the total number of surface receptors (in the model, $R_T = S/Ak_c$, where R_T is the total number

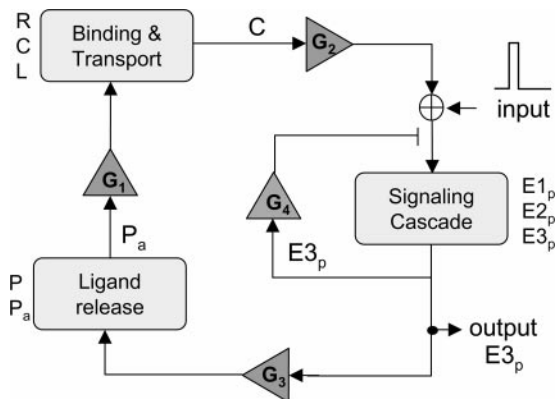


Fig. 5. Block diagram representation of the mathematical model of biochemical events shown in Fig. 1. The model incorporates dynamic interactions between the 3 modules for ligand release, binding and transport, and signaling.

of surface receptors) and the magnitude of extracellular ligand diffusivity.

The extent to which autocrine cells interact with their environment may be estimated by analyzing the statistical properties of the random trajectories followed by autocrine ligands. Let d_{\max} be the maximal distance to which a particle released on the surface of a hemisphere had diffused before being bound by one of the receptors that are uniformly distributed over the surface. Then, d_{\max} defines a random variable with the distribution function dependent on the density of surface receptors (R_T), the extracellular ligand diffusivity, and the forward binding constant. By characterizing the statistical properties of the maximal distances traveled by recaptured autocrine ligands, the distribution function for r_{\max} characterizes the spatial range of autocrine signals. Using the tools for analyzing the extreme properties of Brownian paths (68), we arrive at the following expression for the cumulative distribution function of d_{\max} [we consider only those ligands that have been recaptured by the releasing cell; hence, the distribution function (Eq. 4) asymptotes to 1]

$$P\{d_{\max} \leq d\} = \frac{d(Da + 1)r_{\text{cell}}}{d(Da + 1)r_{\text{cell}} + 1}, \quad \infty > d \geq 0 \quad (4)$$

where $P\{d_{\max} \leq d\}$ denotes the probability that the random variable d_{\max} is less than d .

In Fig. 2C, this distribution function is plotted for the binding parameters characteristic of the EGFR ligand-receptor interaction, 10^5 cell surface receptors (within the range reported for autocrine EGFR systems, i.e., 10^4 – 10^6), and several values of extracellular ligand diffusivity. Computations based on Eq. 4 indicate that, before their recapture, autocrine ligands sample a very small volume; a significant fraction of autocrine ligands is recaptured after traveling only a few micrometers from the cell surface. This spatially restricted character of autocrine loops may account for the initial difficulties in the experimental detection of autocrine ligands in the extracellular medium [13; see also discussion of other experiments in a recent review of EGFR transactivation (28)]. Because the main parameter defining the range of autocrine loops is a Damköhler number (Eq. 2) that depends on the combination of ligand diffusivity, receptor density, and the forward binding constant, all these factors may contribute to tuning the range of autocrine signals.

The results of simulations presented in Fig. 2D show that steady levels of receptor occupancy may be attained within 20 min after the steplike increase in the rate of ligand release. The maximal steady number of surface ligand-receptor complexes predicted by our model is $k_c R_T / k_e$. However, this number can be exceeded in the transient operation of autocrine loops; as illustrated by one of the transients in Fig. 2D, the time course of the number of surface complexes need not be monotonic. Indeed, it has been observed that the high levels of receptor activation, inferred from the levels of receptor tyrosine phosphorylation, can be attained

very quickly after activation of the ligand release system (28).

Protease dynamics. The amount of surface protease in the active form is determined by the balance between the processes for its synthesis, activation, and degradation. Within our model, the total amount of activated protease under steady-state conditions is given by the following expression

$$P_a = \frac{S_P}{k_c} \frac{\mu\nu}{\mu + \nu} \quad (5)$$

where μ and ν depend on the rate constants for the processes of protease constitutive degradation, activation, and degradation of the active form: $\mu = k_c^P / k_e^P$ and $\nu = k_a^P / k_e^P$. In the absence of activation ($\nu = 0$), the total amount of surface protease is S_P / k_c^P . As the rate of protease activation increases, the amount of the active form grows and approaches the asymptote defined by the balance of its synthesis and the endocytosis of the active form: S_P / k_e^P (Fig. 3B).

One can show that whenever the rate constant of constitutive degradation is smaller than the rate constant for degradation of the active form ($\mu < 1$), the total amount of the protease will be a decreasing function of the activation rate constant. Hence, activation of the ligand-releasing protease will be accompanied by its downregulation from the cell surface. Doedens and Black (17) recently demonstrated such stimulation-induced downregulation of the surface metalloprotease for TACE. Because TACE has been implicated in releasing the EGFR ligands (19, 54), this observation is directly related to the operation of the EGFR autocrine loops. In these experiments, it was found that the active form is removed from the surface via an endocytic pathway (36). As the first approach to modeling this problem, we take the rate constant of active protease degradation equal to the endocytic rate constant for the surface ligand-receptor complexes.

The dynamic evolution of the active and inactive forms of the surface protease after a steplike increase in the activation rate constant is presented in Fig. 3, B and D. Although the dynamics of the inactive fraction of the enzyme are always monotonic, the evolution of the active form of the enzyme can exhibit a strong overshoot (i.e., exceed the value to which it eventually settles) before settling to the steady value predicted by Eq. 5. This effect may be important for the operation of autocrine loops: under the conditions of the efficient ligand recapture (see *Transport and Binding*), large-amplitude overshoot in the activity of ligand-releasing enzyme will be registered by the cell surface receptors and relayed to the downstream signaling pathways.

Signaling. Because our model for signaling through the MAPK cascade is closely related to the previously reported models (6, 34, 39), we provide only a brief summary of the intracellular signaling module of the autocrine loop. The input-output behavior of a single stage is critically dependent on the degree of saturation of the enzymes catalyzing the forward and reverse phosphorylation-dephosphorylation reactions (27). When

these enzymes operate close to saturation with respect to their substrates, even a single stage can exhibit sigmoidal input-output dependence. Several stages characterized by the relatively graded input-output behaviors can form a cascade with a very steep input-output response (34, 40). The steady input-output behavior of our modeling cascade is shown in Fig. 4B. The output is negligible below a certain threshold value; past that value, the output increases to its maximal value within a very narrow range of inputs (27, 34). In the cell, this network is under the control of multiple loops that can attenuate or desensitize signaling pathway activity (47). Incorporating the presence of negative feedback in the model affects the input-output behavior: transformation from essentially null to full activation of the last element occurs, now, over a wider range of inputs (Fig. 4B). Multiple stages of the signaling cascade separating its input and output lead to an effective time delay in the dynamic input-output response (not shown). Negative feedback coupled with kinetic time lags can give rise to oscillatory behavior, i.e., periodic oscillations, even for fixed values of external conditions. To distill the dynamic effects mediated by positive-feedback loops (from ligand binding to ligand secretion), we have chosen to work in the region of parameters that does not support oscillatory behavior. Thus, for all the simulations reported below, the input-output behavior of the signaling module is stable.

Computational analysis of the integrated model. We have analyzed the response of our model autocrine loop to pulselike excitations of the signaling cascade (Fig. 6A). Inputs of short duration can be delivered to the MAPK cascade by different means, e.g., by integrins, one of the numerous growth factor receptor systems, or ionizing radiation (10, 30, 47, 50, 75). In our model, activation of the signaling cascade stimulates ligand release and increases receptor occupancy. We have explored the conditions under which this effect leads to a noticeable modulation of the primary excitation. Under the "open-loop" conditions (low number of surface receptors, inhibited receptor or signaling pathway activity), the primary excitations lead to transient, low-amplitude elevation of the activity of the last element of the signaling cascade (lower curves in the transients in Fig. 6, B–D). This primary excitation of the output simply reflects the pulse response of the intracellular signaling cascade. As the number of cell surface receptors is increased, this dynamic response is strongly modulated. Specifically, a secondary excitation of large amplitude and duration appears in the response (Fig. 6B). Simultaneously, the time scale of the dynamic response is dramatically increased from 40 min to several hours. The emergence of long-lasting secondary excitations is critically dependent on the ability of an exogenous signal to cross activate the ligand-releasing protease. See the change in the response shape as a function of the coupling strength between the output of

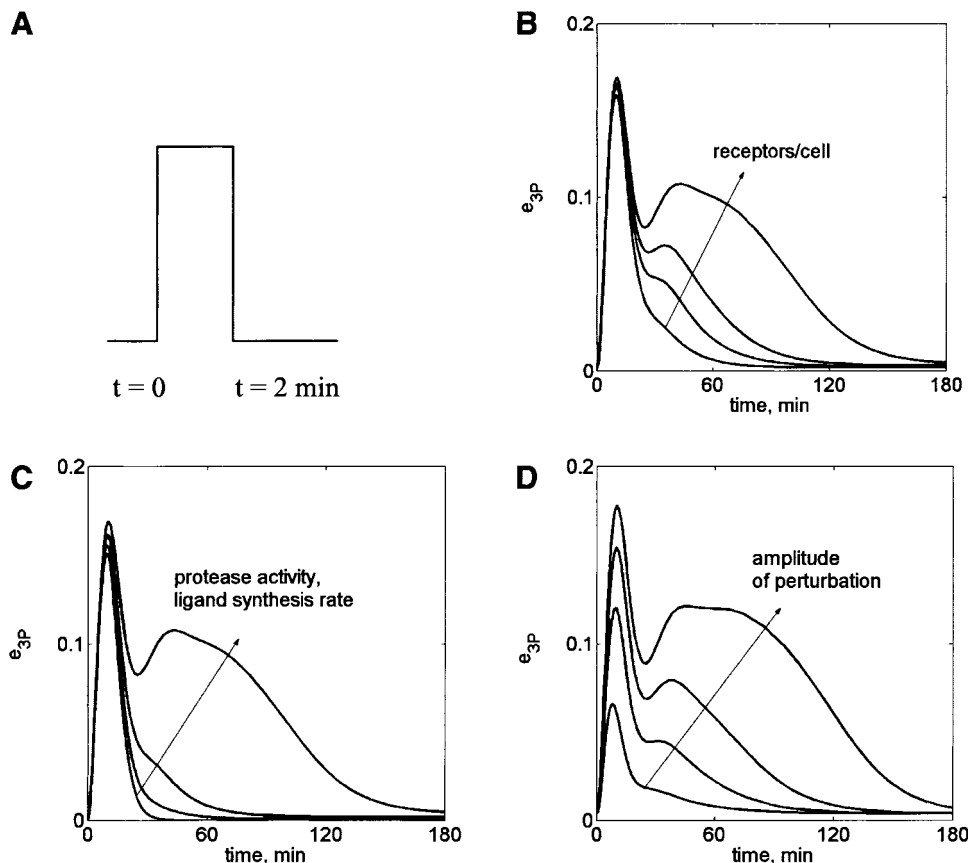


Fig. 6. Autocrine loops can convert transient extracellular inputs to prolonged excitations of the intracellular signaling pathway. A: pulselike, 2-min-long, exogenous perturbation can induce secondary excitations in activity of intracellular signaling that last for several hours. B–D: outputs with secondary excitations are promoted by the high number of cell surface receptors (B) and the high activity of ligand-releasing protease (C). D: amplitude of exogenous stimulus has to be sufficiently high to induce signaling dynamics with secondary excitations. Parameters used in simulations B–D are as follows: $r_{\text{cell}} = 5 \times 10^{-4}$ cm, $D = 10^{-6}$ cm²/s, $k_{\text{off}} = 0.1$ min⁻¹, $k_{\text{on}} = 10^8$ M⁻¹·min⁻¹, $k_e = 0.1$ min⁻¹, $k_c = 0.02$ min⁻¹, $k_s^p = 0.02$ min⁻¹, $k_{a,0}^p = 0.001$ min⁻¹, $k_e^p = 0.1$ min⁻¹, $G_2 = 5 \times 10^{-4}$, $G_3 = 1$, and $G_4 = 1$. Michaelis constants of reactions at the 3 stages of the signaling cascade are the same as in Fig. 4. For transients in B, $G_1 = 0.3$, number of cell surface receptors in the absence of ligand (R_T) = 5×10^4 , and amplitude of the pulselike exogenous stimulus (I_0) = 1, 1.5, 2, and 3.5. For transients in C, $G_1 = 0.3$, $I_0 = 2.5$, and $R_T = 3 \times 10^4$, 4×10^4 , 4.5×10^4 , and 5×10^4 /cell. For transients in D, $I_0 = 2.5$, $R_T = 5 \times 10^4$, and $G_1 = 0, 0.1, 0.2$, and 0.3 .

the signaling cascade and the rate constant of protease activation (Fig. 6C). Hence, the ability of an autocrine cell to recapture endogenous ligands released in response to exogenous stimuli provides a flexible mechanism for tuning the duration of the intracellular signaling response. Our computational analysis shows that, depending on parameters of the integrated network, the amplitude of secondary excitation can be lower and higher than that of the primary excitation (Fig. 7B). The amplitude of the external perturbation has to be sufficiently large to induce the long-lasting response with secondary excitations (Fig. 6D). In this way, the quantitative difference of the transient input, e.g., its input, may be translated into the qualitative differences of the output, such as the number of maxima in the induced response.

A combination of the strong nonlinearity of the intracellular signaling cascade (Fig. 4B) with the positive feedback can result in a phenomenon known as “bistability” (24). Bistability is defined as the ability of the system to exist in two stable configurations at fixed external conditions; selection of a particular stable configuration depends on the history of the system. Indeed, in regimens characterized by stronger coupling between the ligand-releasing protease and ligand secretion rate, larger number of receptors, or weaker gain of the negative feedback in the signaling cascade, the system can exist in one of the two stable (“on” and “off”) configurations (Fig. 7A). The off state is characterized by a low level of signaling, low levels of endogenous ligand production, and a low number of occupied surface receptors. In the on state, large quantities of

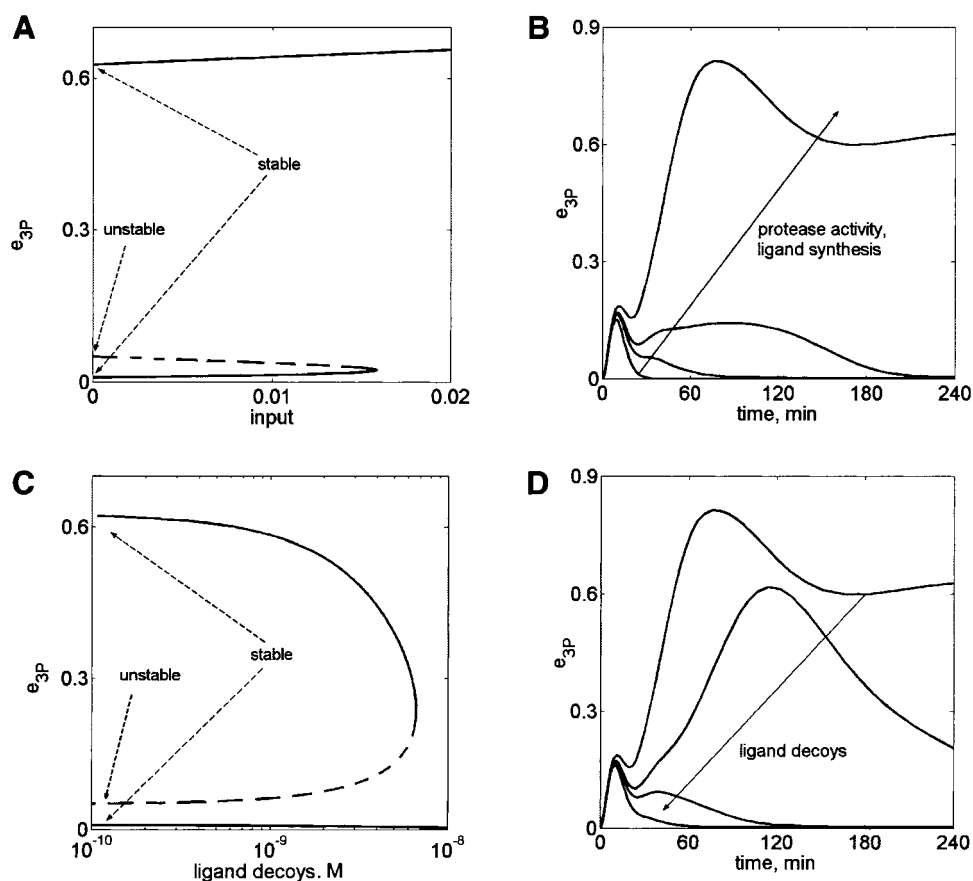


Fig. 7. Memory effect mediated by positive feedback in autocrine loops: transient exogenous input induces sustained activation of the intracellular signaling pathway. **A**: bistability as a basis of memory effects in autocrine loops with positive feedback: steady levels of intracellular signaling activity in a model autocrine loop were computed as a function of (steady) exogenous stimulus. An autocrine loop can exist in one of the two stable steady states. The coexisting steady states are characterized by high and low levels of signaling, even when exogenous input is set to zero. Solid lines, stable stationary states; dashed lines, unstable stationary states. **B**: high levels of ligand synthesis and/or ligand-releasing protease activity promote irreversible activation of intracellular signaling. **C** and **D**: memory effects in autocrine loops are abolished in a dose-dependent way by extracellular addition of antiligand decoys. Bistability at the zero level of exogenous input is destroyed by extracellular addition of antiligand decoys (C). Parameters used in computations are as follows: $R_T = 3 \times 10^4/\text{cell}$, width of pulslike excitation = 2 min, and amplitude (I_0) = 3. For transients in **B**, gain (G_1) between the level of the active form of surface protease and the rate of ligand secretion = 0.0, 0.4, 0.5, and 0.7. For transients in **D**, $G_1 = 0.7$. Antiligand decoys binding the endogenous ligand with forward and reverse rate constants ($k_{\text{off}}^D = 0.1 \text{ min}^{-1}$ and $k_{\text{off}}^D = 10^7 \text{ M}^{-1} \cdot \text{min}^{-1}$) are added at concentrations (B) of 10^{-10} , 10^{-9} , 10^{-7} , and 10^{-8} M. Steady-state diagram (A) is computed at zero concentration of antiligand decoys. All other parameters as in Fig. 4.

signal circulate through the autocrine loop: the cell secretes high levels of ligand and captures a significant fraction of it. The captured ligand further increases the level of intracellular signaling and, as a result, a high secretion rate. In Fig. 7A, the steady input-output behavior of the autocrine loop is shown as a function of the strength of the exogenous input. Below a critical input magnitude the on and off states coexist; above this threshold, the off state can no longer be maintained, and the system switches to the state characterized by the high levels of signaling, receptor occupancy, and ligand release. The autocrine system in a bistable regimen can be flipped between the two steady states by transient inputs. Figure 7B demonstrates that, after a primary excitation, the system can become permanently locked in the on state. Hence, a transient input can induce a permanent transformation of the signaling state of the cell. The switching ability of the transient input is conditional on the autocrine cell's ability to release endogenous ligand (Fig. 7B) and to recapture endogenous ligand (not shown).

To be recaptured by the releasing cell, the secreted ligand clearly must return to the cell surface. Return of autocrine ligands can be prevented by a component of the extracellular medium capable of binding the secreted ligand and removing it from the autocrine loop. The components of the extracellular medium, such as exogenously added antiligand antibodies, may serve as such decoys for autocrine ligands (25); notice that the components of the ECM, such as heparin, may also act as extracellular "sinks" for autocrine ligands (38). We illustrate this by computing the signaling patterns induced in our model autocrine cell when it is placed in the medium with the various concentrations of extracellular decoys. Figure 7C illustrates that the on state of an autocrine loop exists only below a certain threshold concentration of the extracellular decoys that sequester the endogenous ligand. This qualitative change in the steady behavior is mirrored by changes in the dynamic response to a pulselike exogenous stimulus (Fig. 7D). The persistent response is converted to a prolonged transient that is eventually abolished by increasing the concentration of extracellular decoys. This demonstrates the context-dependent signaling capability of autocrine loops: the dynamics of intracellular signaling may be regulated by the composition of the extracellular medium. In contrast to the previously proposed modes of cell signaling, this mode is bidirectional: signals flow into and out of the cell.

Comparison With Experiment

Context-dependent radiation responses of human carcinoma cells. Pulse responses with large- and intermediate-amplitude secondary excitations for EGFR and MAPK signaling were recently reported in studies examining DU145 prostate and A431 squamous carcinoma cells. Similar to the modeling predictions, a pulselike input to the system (a pulse of ionizing radiation) was modulated by the autocrine loop, resulting in complex output (MAPK activity) dynamics. The sig-

nal dynamics are strongly dependent on the actions of the autocrine ligand TGF- α . A description of the experimental protocols is given in APPENDIX B and in Refs. 16, 30, and 58. In the experiments, EGFR-expressing carcinoma cells were exposed to a clinically relevant low dose of ionizing radiation (2 Gy) and assayed for EGFR tyrosine phosphorylation and MAPK activity (16, 30, 58). The response of EGFR tyrosine phosphorylation and MAPK activity consisted of an initial short (0–30 min) primary activation followed by secondary activations of 120–240 min in A431 squamous carcinoma cells (Fig. 8A) and 120–1,440 min in DU145 prostate carcinoma cells (not shown). In both cell types, the secondary excitation of MAPK could be completely abolished by interrupting the TGF- α -EGFR autocrine loop. This was demonstrated experimentally by inhibiting EGFR tyrosine kinase activity (not shown) and by adding antibodies absorbing the se-

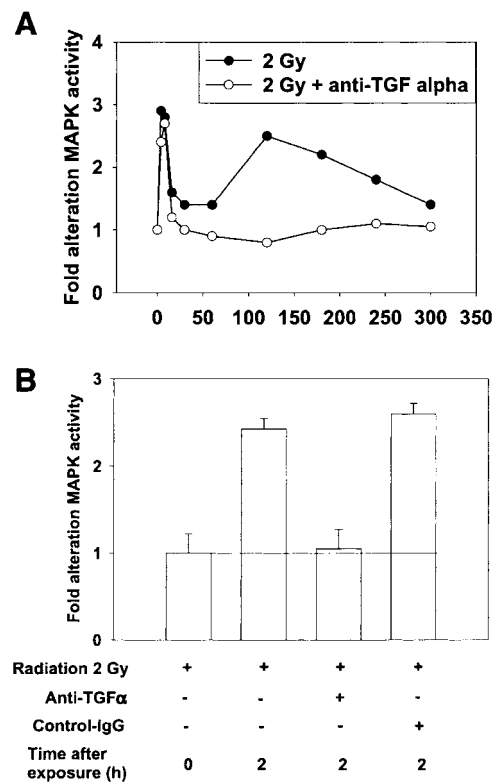


Fig. 8. Radiation causes a biphasic activation of the MAPK pathway in autocrine carcinoma cells; secondary activation of the MAPK pathway is dependent on cleavage and release of TGF- α . **A**: cells were irradiated, and MAPK activity was determined as described previously (16, 30). In the indicated experiments, anti-TGF- α antibody (1 μ g/ml media) was added before irradiation. Cells were lysed, portions (~100 μ g) from each plate were used to immunoprecipitate MAPK, and immune-complex kinase assays were performed (16, 30). Data are from a representative experiment ($n = 5$). **B**: A431 cells were irradiated, medium was removed from irradiated cells 120 min after exposure, and anti-TGF- α antibody or control antibody was added to the recovered medium. Isolated medium was incubated with antibody for 60 min, and then nonirradiated cells were added. After 5 min, the plates were aspirated and snap frozen, and MAPK activity was determined after immunoprecipitation (16, 30). MAPK activity data are shown as fold increases in 32 P incorporation into myelin basic protein substrate and are normalized to activity at *time 0*. Values are means \pm SE of 3 independent experiments.

creted TGF- α (Fig. 8A). When the medium from the irradiated cells was transferred to nonirradiated cells, 2 h after exposure, a comparable MAPK activation was induced in the nonirradiated cells that was dependent on soluble TGF- α in the transferred medium (Fig. 8B). To summarize, experiments in Fig. 8 demonstrate that the primary exogenous stimulus (radiation, in this particular case) activates autocrine loops and that this activation depends on the composition of the extracellular medium. Figure 8A shows that secondary excitation in MAPK activity disappears when radiation stimulates the cells placed in the medium containing antiligand antibodies. A complementary experiment in Fig. 8B shows that medium from the irradiated cells can stimulate MAPK in the nonirradiated cells; this effect is abolished when antiligand antibodies are added to the conditioned medium.

Enhanced ligand secretion and prolonged MAPK activity in the irradiated cells could be abolished when the A431 squamous carcinoma cells were treated with PD-98059, an inhibitor of the enzyme MEK1/2, acting upstream of MAPK in the kinase cascade. In these cells, the basal release of TGF- α over a 3-h period was ~ 60 pg/mg total cell protein. Irradiation (2 Gy) increased TGF- α release by $\sim 80\%$; this release was blocked when irradiated cells were incubated with the MEK1/2 inhibitor PD-98059 (data not shown). Similar data for regulation of TGF- α release, using ligand

stimulation of the EGFR-MAPK system, have been reported in other cell types (16, 30, 58). Collectively, these experiments support an MAPK-mediated positive-feedback loop between ligand binding and ligand release.

Interestingly, the dynamics of MAPK signaling observed in these irradiated autocrine cells indicate the presence of the multiple steady states (16, 30, 58). As in our computational study, transient input seems to permanently lock MAPK in the active on state in DU145 cells, whereas in A431 cells the duration of secondary MAPK activation was only 2–3 h (16, 30, 45). The greater secondary activation of MAPK in DU145 cells may be explained because these cells have a genetic rearrangement of the TGF- α gene, resulting in its triplication (11), and thus express more autocrine ligand than A431 cells.

DISCUSSION

We have developed a mechanistic model of autocrine loops in the EGFR system (Fig. 9). The model accounts for the dynamic interaction of ligand release, extracellular transport, receptor binding, and signaling through the Ras-MAPK pathway. Our computational analysis demonstrates that autocrine loops with positive feedback allow cells to modulate the amplitude and the duration of the signaling response to external stimuli.

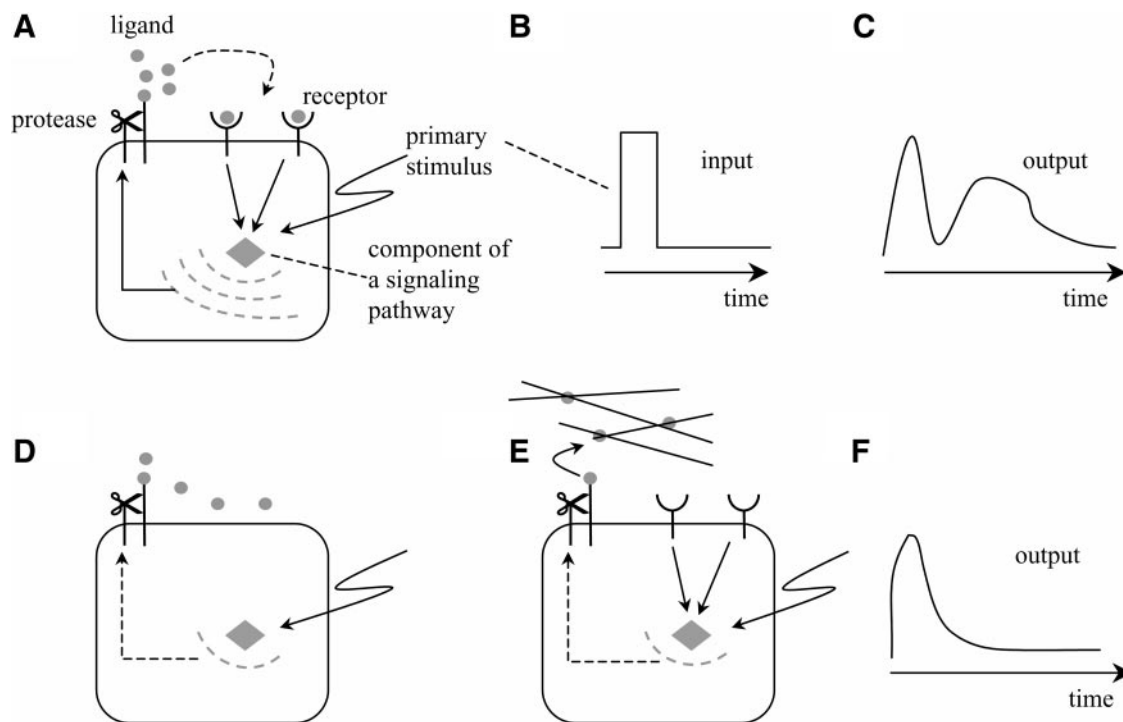


Fig. 9. Concept of context-dependent cell signaling mediated by positive feedback in autocrine loops. Amplitude and duration of activation of an intracellular signaling cascade by exogenous stimulus depend on the primary stimulus, its ability to activate the ligand-release system, and the ability of the cell to recapture endogenous ligands. Autocrine loop in the “on” state (A) converts transient external perturbation (B) to a long-lasting and dynamic transient of the intracellular signaling (C). Autocrine loop is interrupted when the cell has a low number of surface receptors (D) or when the endogenous ligands are captured by components of the cellular microenvironment (E). In this case, the exogenous stimulus is incapable of inducing long-lasting or sustained activation of the intracellular signaling circuitry (F).

Specifically, a pulsatile input lasting only several minutes induces a signaling transient that lasts for several hours. Furthermore, transient inputs can permanently leave the autocrine loop in the on state, characterized by the high signaling level. Both of these features are demonstrated in the study of the EGFR autocrine loops in human carcinoma cells (see also Refs. 16, 30, and 58). In these cells, a 1-min pulse of γ -radiation results in TGF- α release and leads to complex MAPK dynamics on the time scale of hours. Sustained activation of the ERK1/2 MAPK in the EGFR-TGF- α autocrine loop has also been detected in cancerous pancreatic cells and suggested to be a cause of their serum-free growth (52). We have focused on the positive feedback that operates exclusively at the level of signaling. Under the additional control of feedbacks acting at the level of gene expression, the nonlinear effects reported here are likely to become even more pronounced.

We have demonstrated that dynamics of autocrine loops with positive feedback are governed jointly by the intracellular and extracellular processes. In particular, interactions of secreted ligands with components of the extracellular environment are translated into the dynamics of the intracellular signaling. On the basis of our computational and experimental studies, we propose that the EGFR autocrine loop with positive feedback is a module for context-dependent signal processing. Two cells equipped with the same intracellular signaling capabilities but different in their ability to release and recapture autocrine ligands may respond differently to the same external input. In this work, the extracellular context, characterized by the presence or absence of antiligand antibodies, is reflected in the MAPK dynamics and defines cell response to radiation: the presence or absence of long-lived MAPK excitations mediated by the EGFR-TGF- α autocrine loop defines whether the irradiated cell survives or dies. Further supporting our model of context-dependent signaling is a recent experiment in which the EGFR autocrine loop regulates the ability of a G protein agonist (thrombin) to induce cell migration (38). There, stimulation of the EGFR by the heparin-binding EGF, released in response to exogenous thrombin, was necessary for thrombin-induced migration of rat and baboon smooth muscle cells; interruption of autocrine signaling by soluble heparin or antiligand antibodies abrogated thrombin-induced cell motility.

On the basis of our computational studies and the experiments reporting the effect of exogenously added soluble antiligand antibodies or other factors interacting with autocrine ligands, we suggest that the composition of the ECM can affect signaling dynamics via a similar bidirectional mechanism. Mathematical analysis of this hypothesis would involve changing the freely diffusing ligand decoys in our model to immobile extracellular components interacting with the secreted ligands. Merely as suggestive examples, we outline experiments that could potentially support or refute this extended hypothesis. A technique for patterning of the ECM components could be used to create a surface gradient in the concentration of heparin; this pat-

terned substrate could then be used for migration studies of autocrine cells expressing heparin-binding EGF. Our extended hypothesis would predict that the static gradient of heparin would lead to chemotaxis of autocrine cells toward the higher concentration of heparin; the effect should be abolished by the addition of antibodies blocking the surface receptors. If successful, this experiment would demonstrate that the composition of the ECM can affect cell physiology (in this case, cell migration) by perturbing the operation of autocrine loops. Presumably, similar studies could be performed using other ECM components such as collagen or fibronectin. Another experiment, aimed at demonstrating this effect at the level of cell signaling, would follow the MAPK dynamics induced by exogenously added growth factors in cells plated on substrates with different levels of heparin.

A critical question arising in the design of anticancer therapies targeting autocrine loops is how to optimally select particular components within a signaling network to be targeted for pharmacological inhibition. Another question is how to choose among multiple antireceptor and antiligand antibodies, tyrosine kinase inhibitors, inhibitors of membrane-associated proteases that release autocrine ligands, and inhibitors of the downstream signaling components. Rational design of therapies that target systems as complex as autocrine loops may benefit from the further development and validation of our model. In particular, a combination of further modeling and parameter estimation techniques is required to convert our model to a practical tool for the analysis and eventually the design of radiation responses of autocrine cells. Within the last 2 yr, several groups have reported time-resolved measurements of reactive oxygen species (ROS) (46) generation and intracellular signaling activation in response to ionizing radiation (for review see Refs. 42 and 59). These experiments have identified several mechanisms by which radiation can impact the autocrine loop. By generating ROS, ionizing radiation can potentially inhibit receptor tyrosine phosphatases and cause ligand-independent receptor activation; at the same time, ROS can activate ligand-releasing proteases (74) and the components of the intracellular signaling pathways, such as Raf-1 (see Ref. 59 and references therein). A mechanistic description of these effects will be a natural extension of the model presented here. In the present version of the model, the signaling activity of the ligand-receptor complex ceases with its internalization, and the rate of ligand recycling is set to zero. The model can be made more quantitative by accounting for the effects of receptor and ligand recycling and signaling from early endosomes (3, 9, 22, 32, 65, 67, 71, 73) and for the effects of signaling through other pathways stimulated by the EGFR (33, 57, 69). Given the fact that autocrine signaling through the EGFR loops has been identified as one of the major cytoprotective mechanisms determining the success of cancer radiotherapy (1, 35, 58), we believe that this modeling effort is necessary.

APPENDIX A

Model Equations

Binding and transport. We consider the axially symmetrical spatial distribution of ligand around the cell. The governing equations and boundary conditions are

$$\frac{\partial \bar{L}}{\partial t} = D \left(\frac{\partial^2 \bar{L}}{\partial r^2} + \frac{2}{r} \frac{\partial \bar{L}}{\partial r} \right) - k_{\text{on}}^D \bar{L}^B B + k_{\text{off}}^D \bar{L}^B \quad (\text{A1})$$

$$\frac{\partial \bar{L}^B}{\partial t} = D \left(\frac{\partial^2 \bar{L}^B}{\partial r^2} + \frac{2}{r} \frac{\partial \bar{L}^B}{\partial r} \right) + k_{\text{on}}^D \bar{L}^B B - k_{\text{off}}^D \bar{L}^B \quad (\text{A2})$$

$$\frac{dR_s}{dt} = -k_{\text{on}} R_s \bar{L}(r_{\text{cell}}) + k_{\text{off}} C + s - k_c R_s \quad (\text{A3})$$

$$\frac{dC}{dt} = k_{\text{on}} R_s \bar{L} - k_{\text{off}} C - k_c C \quad (\text{A4})$$

$$D \frac{\partial \bar{L}(r_{\text{cell}}, t)}{\partial r} = -q + k_{\text{on}} R_s \bar{L} - k_{\text{off}} C, \quad \bar{L}(\infty, t) = 0 \quad (\text{A5})$$

$$\bar{L}^B(\infty, t) = 0, \quad D \frac{\partial \bar{L}^B(r_{\text{cell}}, t)}{\partial r} = 0 \quad (\text{A6})$$

In the present version of the model, the diffusivity of the ligand (D) does not depend on its association with an anti-ligand antibody. The system of equations is rendered dimensionless by the following transformations

$$\rho = \frac{r}{r_{\text{cell}}}, \quad \tau = k_{\text{off}} t, \quad \bar{L} = \frac{L}{K_d}, \quad (\text{A7})$$

$$\bar{L}^B = \frac{L^B}{K_d}, \quad \bar{C} = \frac{C_s}{s/k_c}, \quad \bar{R} = \frac{R_s}{s/k_c}$$

The cell radius scales the coordinate; the time (t) is scaled by the inverse dissociation rate constant; extracellular ligand concentrations are scaled by the equilibrium binding constant; the surface densities of free and occupied receptors are scaled by the density of receptors in the absence of ligand ($R_T \equiv s/k_c$). The rescaled problem takes the following form (see RESULTS for definitions of dimensionless groups Au , Da , δ , and γ)

$$\epsilon \frac{\partial \bar{L}}{\partial \tau} = \frac{\partial^2 \bar{L}}{\partial \rho^2} + \frac{2}{\rho} \frac{\partial \bar{L}}{\partial \rho} - k^+ \bar{L} + k^- \bar{L}^B \quad (\text{A8})$$

$$\epsilon \frac{\partial \bar{L}^B}{\partial \tau} = \frac{\partial^2 \bar{L}^B}{\partial \rho^2} + \frac{2}{\rho} \frac{\partial \bar{L}^B}{\partial \rho} + k^+ \bar{L} - k^- \bar{L}^B \quad (\text{A9})$$

$$\frac{d\bar{R}}{d\tau} = -\bar{R} \bar{L}(1) + \gamma(1 - \bar{R}) + \bar{C} \quad (\text{A10})$$

$$\frac{d\bar{C}}{d\tau} = \bar{R} \bar{L} - \frac{1}{1 - \delta} \bar{C} \quad (\text{A11})$$

$$\frac{\partial \bar{L}(1, \tau)}{\partial \rho} = -Au + \delta Da \bar{R} \bar{L}, \quad \bar{L}(\infty, \tau) = 0 \quad (\text{A12})$$

$$\frac{\partial \bar{L}^B(1, \tau)}{\partial \rho} = 0, \quad \bar{L}^B(\infty, \tau) = 0 \quad (\text{A13})$$

The time scale of extracellular diffusion is defined by $\epsilon = r_{\text{cell}}^2 k_{\text{off}} / D$. Dimensionless binding constants, k^+ and k^- , reflect the strength with which the secreted ligand is bound by the extracellular component: $k_+ = k_{\text{on}}^B Br_{\text{cell}}^2 / D$ and $k_- = k_{\text{off}}^B r_{\text{cell}}^2 / D$. For high values of the secreted growth factor diffusivity ($\epsilon \ll 1$), concentrations of soluble species evolve on

the time scale that is much shorter than that of surface receptors and ligand-receptor complexes. In this regimen, the binding/transport model can be simplified by using a steady-state approximation for the concentration of endogenous ligand; we can solve for the value of this concentration at the surface of our autocrine cell

$$\bar{L}(1) = \frac{Au + Da\bar{C}}{W + Da\bar{R}} \quad (\text{A14})$$

where W depends on the composition of the extracellular medium and the rate constants of the forward and reverse binding processes: $W = [1 + (k_+ + k_-)^{1/2}] / [1 + k_- / (k_+ + k_-)^{1/2}]$. The pseudo-steady-state approximation (Eq. A14) for the concentration of secreted ligand leads to the following model for the dynamics of free and bound cell surface receptors

$$\frac{d\bar{R}}{d\tau} = -\bar{R} \frac{Au + Da\bar{C}}{1 + Da\bar{R}} + \gamma(1 - \bar{R}) + \bar{C} \quad (\text{A15})$$

$$\frac{d\bar{C}}{d\tau} = \bar{R} \frac{Au + Da\bar{C}}{W + Da\bar{R}} - \frac{\bar{C}}{1 - \delta} \quad (\text{A16})$$

More subtle details of receptor binding and trafficking, such as dimerization, stoichiometric saturation of internalization, and endosomal sorting to recycling, could be easily incorporated into the model.

Protease dynamics. The model is formulated in terms of P and P_a

$$\frac{dP}{dt} = S_p - k_c^P P - k_a^P P \quad (\text{A17})$$

$$\frac{dP_a}{dt} = k_a^P P - k_c^P P_a \quad (\text{A18})$$

After rescaling according to

$$\bar{P} = k_c^P P / S_p, \quad \bar{P}_a = k_c^P P_a / S_p, \quad \mu = k_c^P / k_e^P, \quad \nu = k_a^P / k_e^P, \quad \tau = tk_e^P \quad (\text{A19})$$

the system is converted to its dimensionless form

$$\frac{d\bar{P}}{d\tau} = \mu(1 - \bar{P}) - \nu\bar{P} \quad (\text{A20})$$

$$\frac{d\bar{P}_a}{d\tau} = \nu\bar{P} - \bar{P}_a \quad (\text{A21})$$

Signaling cascade. Let e_{1P} , e_{2P} , and e_{3P} denote the dimensionless (scaled by the total amount of the enzyme) concentrations of the active ("phosphorylated") form of the enzymes. The model for dynamics of e_{1P} , e_{2P} , and e_{3P} has the following form

$$\frac{de_{1P}}{dt} = \frac{I(t)}{1 + G_4 e_{3P}} \frac{V_{\text{max},1}(1 - e_{1P})}{K_{m,1} + (1 - e_{1P})} - \frac{V_{\text{max},2} e_{1P}}{K_{m,2} + e_{1P}} \quad (\text{A22})$$

$$\frac{de_{2P}}{dt} = \frac{V_{\text{max},3} e_{1P}(1 - e_{2P})}{K_{m,3} + (1 - e_{2P})} - \frac{V_{\text{max},4} e_{2P}}{K_{m,4} + e_{2P}} \quad (\text{A23})$$

$$\frac{de_{3P}}{dt} = \frac{V_{\text{max},5} e_{2P}(1 - e_{3P})}{K_{m,5} + (1 - e_{3P})} - \frac{V_{\text{max},6} e_{3P}}{K_{m,6} + e_{3P}} \quad (\text{A24})$$

In this form, the equilibrium Michaelis constants ($K_{m,i}$) are rescaled by the total amount of enzyme at a given stage of the cascade; V_{max} is maximal reaction velocity.

Coupled system. The input to the signaling cascade is given by $I = I_0 + G_2 R_T \bar{C}$, where I_0 denotes (possibly time-dependent) input to the signaling network, independent of endog-

enous ligand, and G_2 quantifies the efficiency with which occupied receptor stimulates the input to the signaling cascade. The (scaled) rate of protease activation is given by $\nu = \nu_0 + G_3 e_{3p}$, where ν is the rate of activation mediated by "MAPK-independent" processes. Finally, the rate of ligand secretion is $Q \sim Au = G_1 P_a$. The integrated model of an autocrine cell then becomes (the units of time are now the same in all 3 modules of our autocrine loop)

$$\frac{de_{1p}}{dt} = \frac{I_0(t) + G_2 R_T \bar{C}}{1 + G_4 e_{3p}} \frac{1 - e_{1p}}{K_{m,1} + (1 - e_{1p})} - \frac{V_{\max,2} e_{1p}}{K_{m,2} + e_{1p}} \quad (A25)$$

$$\frac{de_{2p}}{dt} = \frac{V_{\max,3} e_{1p} (1 - e_{2p})}{K_{m,3} + (1 - e_{2p})} - \frac{V_{\max,4} e_{2p}}{K_{m,4} + e_{2p}} \quad (A26)$$

$$\frac{de_{3p}}{dt} = \frac{V_{\max,5} e_{2p} (1 - e_{3p})}{K_{m,5} + (1 - e_{3p})} - \frac{V_{\max,6} e_{3p}}{K_{m,6} + e_{3p}} \quad (A27)$$

$$\frac{d\bar{P}}{dt} = k_c^p (1 - \bar{P}) - (k_{a,\text{base}}^p + G_3 k_e^p e_{3p}) \bar{P} \quad (A28)$$

$$\frac{d\bar{P}_a}{dt} = (k_{a,\text{base}}^p + G_3 k_e^p e_{3p}) \bar{P} - k_e^p \bar{P}_a \quad (A29)$$

$$\frac{d\bar{R}}{dt} = -k_{\text{off}} \bar{R} \frac{G_1 \bar{P}_a + \text{Da} \bar{C}}{W + \text{Da} \bar{R}} + k_c (1 - \bar{R}) + k_{\text{off}} \bar{C} \quad (A30)$$

$$\frac{d\bar{C}}{dt} = k_{\text{off}} \bar{R} \frac{G_1 \bar{P}_a + \text{Da} \bar{C}}{W + \text{Da} \bar{R}} - (k_e + k_{\text{off}}) \bar{C} \quad (A31)$$

APPENDIX B

Materials and Experimental Methods

Reagents. Anti-p42^{MAPK} (sc-154AC) was obtained from Santa Cruz Biotechnology (Santa Cruz Biotechnologies, CA), the neutralizing monoclonal antibody to TGF- α (Ab-3) and control antibody to TFIID (Ab-2) from Calbiochem (San Diego, CA), and [γ -³²P]ATP from NEN. The enzyme-linked immunosorbent assay to measure TGF- α release was purchased from Oncogene Research Products (San Diego, CA), and studies were performed according to the manufacturer's instructions. Other materials were as described previously (16, 30).

Culture of A431 cells. A431-TR25-EGFR antisense cells were plated at a density of 3.2×10^4 cells/cm² and cultured for 4 days in RPMI 1640 medium supplemented with 5% (vol/vol) fetal calf serum at 37°C in 95% (vol/vol) air-5% (vol/vol) CO₂, as described previously (16). Cells were cultured in reduced-serum (0.5% vol/vol) medium for 2 h before irradiation. Cells were at ~70% confluency at the time of irradiation.

Treatment of cells with ionizing radiation and cell homogenization. Cells were cultured as described above and serum starved for 12 h before irradiation (16). In the experiments, anti-TGF- α antibody (1 μ g/ml medium) was added 60 min before irradiation. For media transfer assays, anti-TGF- α antibody (2 μ g) was added to recovered medium 120 min after irradiation, and the medium was incubated with antibody for 60 min before further use. A control antibody to the transcriptional regulator TFIID corresponding to the same monoclonal antibody subtype (IgG2) as the anti-TGF- α antibody was used as a control. Cells were irradiated using a ⁶⁰Co source at 1.8 Gy/min, to a total of 2 Gy. *Time 0* is the time at which exposure to radiation ceased. After radiation treatment, cells were incubated for specified times, and then the medium was aspirated and snap frozen at -70°C on dry ice. Cells were homogenized as described previously (16, 30).

Immunoprecipitation and assay of MAPK activity. Immunoprecipitates were incubated with [γ -³²P]ATP and myelin basic protein, as described elsewhere (16, 30). ³²P incorporation into myelin basic protein was quantified by liquid scintillation spectroscopy, as described previously (16, 30).

Data analysis. The effects of various treatments were compared using one-way analysis of variance and a two-tailed *t*-test. Differences with $P < 0.05$ were considered statistically significant. Values are means \pm SE of multiple individual points from multiple separate experiments.

This work was partially funded by Defense Advanced Research Projects Agency Grant MDA972-00-1-0030 to D. A. Lauffenburger and National Institute of General Medical Sciences Postdoctoral Fellowship F32 GM-20847 to S. Y. Shvartsman. P. Dent is funded by National Institutes of Health Grants R01 DK-52825 and R01 CA-88906 and US Department of Defense Grant BC98-0148. A. Yacoub is funded by the Department of Radiation Oncology, Virginia Commonwealth University, and is a postdoctoral fellow in the laboratory of Dr. M. P. Hagan.

REFERENCES

1. Akimoto T, Hunter N, Buchmiller L, Mason K, Ang K, and Milas L. Inverse relationship between the epidermal receptor expression and radiocurability of murine carcinomas. *Clin Cancer Res* 5: 2884-2890, 1999.
2. Asthagiri A, Nelson C, Horwitz A, and Lauffenburger D. Quantitative relationship among integrin-ligand binding, adhesion, and signaling via focal adhesion kinase and extracellular signal-regulated kinase 2. *J Biol Chem* 274: 119-127, 1999.
3. Bao J, Alroy I, Waterman H, Schejter E, Brodie C, Grunberg J, and Yarden Y. Threonine phosphorylation diverts internalized epidermal growth factor receptors from a degradative pathway to the recycling endosome. *J Biol Chem* 275: 26178-26186, 2000.
5. Berg HC and Purcell EM. Physics of chemoreception. *Biophys J* 20: 193-219, 1977.
6. Bhalla U and Iyengar R. Emergent properties of networks of biological signaling pathways. *Science* 283: 339-340, 1999.
7. Blobel C. Remarkable roles of proteolysis on and beyond the cell surface. *Curr Opin Cell Biol* 12: 606-612, 2000.
8. Brighman F and Fell D. Differential feedback regulation of the MAPK cascade underlies the quantitative differences in EGF and NGF signaling in PC12 cells. *FEBS Lett* 482: 169-174, 2000.
9. Burke P, Schooler K, and Wiley H. Regulation of epidermal growth factor receptor signaling by endocytosis and intracellular trafficking. *Mol Cell Biol* 12: 1897-1910, 2001.
10. Carpenter G. Employment of the epidermal growth factor receptor in growth factor-independent signaling pathways. *J Cell Biol* 146: 697-702, 1999.
11. Ching K, Ramsey E, Pettigrew N, D'Cunha R, Jason M, and Dodd J. Expression of mRNA for epidermal growth factor, transforming growth factor- α , and their receptors in human prostate tissue and cell lines. *Mol Cell Biochem* 126: 151-158, 1993.
12. Ciardiello F. Epidermal growth factor receptor tyrosine kinase inhibitors as anticancer agents. *Drugs* 60: 25-32, 2000.
13. Daub H, Weiss F, Wallasch C, and Ullrich A. Role of transactivation of the EGF receptor in signalling by G-protein-coupled receptors. *Nature* 379: 557-560, 1996.
14. Deen WM. *Analysis of Transport Phenomena*. New York: Oxford University Press, 1998.
15. Dempsey P and Coffey R. Basolateral targeting and efficient consumption of transforming growth factor- α when expressed in Madin-Darby kidney cells. *J Biol Chem* 269: 16878-16889, 1994.
16. Dent P, Reardon D, Park J, Bowers G, Logsdon C, Valerie K, and Schmidt-Ullrich R. Radiation-induced release of transforming growth factor- α activates the epidermal growth factor receptor and mitogen-activated protein kinase pathway in carcinoma cells, leading to increased proliferation and protection from radiation-induced cell death. *Mol Biol Cell* 10: 2493-2506, 1999.

17. **Doedens JR and Black RA.** Stimulation-induced down-regulation of tumor necrosis factor- α -converting enzyme. *J Biol Chem* 275: 14598–14607, 2000.
18. **Domagala T, Konstantopoulos N, Smyth F, Jorissen R, Fabri L, Geleick D, Lax I, Schlessinger J, Sawyer W, Howlett G, Burgess A, and Nice E.** Stoichiometry, kinetic and binding analysis of the interaction between epidermal factor (EGF) and the extracellular domain of the EGF receptor. *Growth Factors* 18: 11–29, 2000.
19. **Dong JY, Opresko LK, Dempsey PJ, Lauffenburger DA, Coffey RJ, and Wiley HS.** Metalloprotease-mediated ligand release regulates autocrine signaling through the epidermal growth factor receptor. *Proc Natl Acad Sci USA* 96: 6235–6240, 1999.
20. **Dong JY and Wiley HS.** Trafficking and proteolytic release of epidermal growth factor receptor ligands are modulated by their membrane-anchoring domains. *J Biol Chem* 275: 557–564, 1999.
21. **Dowd CJ, Cooney CL, and Nugent MA.** Heparan sulfate mediates bFGF transport through basement membrane by diffusion with rapid reversible binding. *J Biol Chem* 274: 5236–5244, 1999.
22. **Ettenberg SA, Magnifico A, Cuello M, Nau MM, Rubinstein YR, Yarden Y, Weissman AM, and Lipkowitz S.** Cbl-b-dependent coordinated degradation of the epidermal growth factor receptor signaling complex. *J Biol Chem* 276: 27677–27684, 2001.
23. **Fan HZ and Derynck R.** Ectodomain shedding of TGF- α and other transmembrane proteins is induced by receptor tyrosine kinase activation and MAP kinase signaling cascades. *EMBO J* 18: 6962–6972, 1999.
24. **Ferrell JJ and Machleder E.** The biochemical basis of an all-or-none cell fate switch in *Xenopus* oocytes. *Science* 280: 895–898, 1998.
25. **Forsten KE and Lauffenburger DA.** Interrupting autocrine ligand-receptor binding: comparison between receptor blockers and ligand decoys. *Biophys J* 63: 857–861, 1992.
26. **Gechtman Z, Alonso JL, Raab G, Ingber DE, and Klagsbrun M.** The shedding of membrane-anchored heparin-binding epidermal-like growth factor is regulated by the Raf/mitogen-activated protein kinase cascade and by cell adhesion and spreading. *J Biol Chem* 274: 28828–28835, 1999.
27. **Goldbeter A and Koshland DJ.** An amplified sensitivity arising from covalent modification in biological systems. *Proc Natl Acad Sci USA* 78: 6840–6844, 1981.
28. **Gschwind A, Zwick E, Prenzler N, Leserer M, and Ullrich A.** Cell communication networks: epidermal growth factor receptor transactivation as the paradigm for interreceptor signal transmission. *Oncogene* 20: 1594–1600, 2001.
29. **Guan R, Zhang Y, Jiang J, Baumann C, Black R, Baumann G, and Frank S.** Phorbol ester- and growth factor-induced growth hormone (GH) proteolysis and GH-binding protein shedding: relationship to GH receptor downregulation. *Endocrinology* 142: 1137–1147, 2001.
30. **Hagan M, Wang L, Hanley JR, Park JS, and Dent P.** Ionizing radiation-induced mitogen-activated protein (MAP) kinase activation in DU145 prostate carcinoma cells: MAP kinase inhibition enhances radiation-induced cell killing and G₂/M-phase arrest. *Radiat Res* 153: 371–383, 2000.
31. **Halfon M, Carmena A, Gisselbrecht S, Sackerson C, Jimenez F, Baylies M, and Michelson A.** Ras pathway specificity is determined by the integration of multiple signal-activated and tissue-restricted transcription factors. *Cell* 103: 63–74, 2000.
32. **Haugh J, Huang A, Wiley H, Wells A, and Lauffenburger D.** Internalized epidermal growth factor receptors participate in the activation of p21^{ras} in fibroblasts. *J Biol Chem* 274: 34350–34360, 1999.
33. **Haugh J, Wells A, and Lauffenburger D.** Mathematical modeling of epidermal growth factor receptor signaling through the phospholipase C pathway: mechanistic insights and predictions for molecular interventions. *Biotechnol Bioeng* 70: 225–238, 2000.
34. **Huang C and Ferrell JJ.** Ultrasensitivity in the mitogen-activated protein kinase cascade. *Proc Natl Acad Sci USA* 93: 10078–10083, 1996.
35. **Huang S and Harari P.** Modulation of radiation response after epidermal growth factor blockade in squamous cell carcinomas: inhibition of damage repair, cell cycle kinetics, and tumor angiogenesis. *Clin Cancer Res* 6: 2166–2174, 2000.
36. **Hunter T.** The Croonian Lecture 1997. The phosphorylation of proteins on tyrosine: its role in cell growth and disease. *Philos Trans R Soc Lond B Biol Sci* 353: 583–605, 1998.
37. **Hunter T.** Signaling—2000 and beyond. *Cell* 100: 113–127, 2000.
38. **Kalmes A, Vesti B, Daum G, Abraham J, and Clowes A.** Heparin blockade of thrombin-induced smooth muscle cell migration involves inhibition of epidermal growth factor (EGF) receptor transactivation by heparin-binding EGF-like growth factor. *Circ Res* 87: 92–98, 2000.
39. **Kholodenko B.** Negative feedback and ultrasensitivity can bring about oscillations in the mitogen-activated protein kinase cascades. *Eur J Biochem* 267: 1583–1588, 2000.
40. **Kholodenko B, Hoek J, Westerhoff H, and Brown G.** Quantification of information transfer via cellular signal transduction pathways. *FEBS Lett* 419: 430–434, 1997.
41. **Kholodenko BN, Demin OV, Moehren G, and Hoek JB.** Quantification of short-term signaling by the epidermal growth factor receptor. *J Biol Chem* 274: 30169–30181, 1999.
42. **Knebel A, Bohmer F, and Herrlich P.** Radiation-induced signal transduction. *Methods Enzymol* 319: 255–272, 2000.
43. **Lauffenburger D and Linderman J.** *Receptors: Models for Binding, Trafficking, and Signalling.* New York: Oxford University Press, 1993.
44. **Lauffenburger DA, Oehrtman GT, Walker L, and Wiley HS.** Real-time quantitative measurement of autocrine ligand binding indicates that autocrine loops are spatially localized. *Proc Natl Acad Sci USA* 95: 15368–15373, 1998.
45. **Lavoie J, Rivard N, L'Allemain G, and Pouyssegur JA.** A temporal and biochemical link between growth factor-activated MAP kinases, cyclin D1 induction and cell cycle entry. *Prog Cell Cycle Res* 2: 49–58, 1996.
46. **Leach J, Van Tuyle G, Lin P, Schmidt-Ullrich R, and Mikkelsen R.** Ionizing radiation-induced, mitochondria-dependent generation of reactive oxygen/nitrogen. *Cancer Res* 61: 3894–3901, 2001.
47. **Lewis T, Shapiro P, and Ahn N.** Signal transduction through MAP kinase cascades. *Adv Cancer Res* 74: 49–139, 1998.
48. **Marshall CJ.** Specificity of receptor tyrosine kinase signaling: transient versus sustained extracellular signal-regulated kinase activation. *Cell* 80: 179–185, 1995.
49. **Massague J and Pandiella A.** Membrane-anchored growth factors. *Annu Rev Biochem* 62: 515–541, 1993.
50. **Moghal M and Sternberg PW.** Multiple positive and negative regulators of signaling by the EGF receptor. *Curr Opin Cell Biol* 11: 190–196, 1999.
51. **Montero J, Yuste L, Diaz-Rodriguez E, Espasis-Ogando A, and Pandiella A.** Differential shedding of transmembrane neuregulin isoforms by tumor necrosis factor- α -converting enzyme. *Mol Cell Neurosci* 16: 631–648, 2000.
52. **Murphy L, Cluck M, Lovas S, Otvos F, Murphy R, Schally A, Permert J, Larsson J, Knezetic J, and Adrian T.** Pancreatic cancer cells require and EGF receptor-mediated autocrine pathway for proliferation under serum-free conditions. *Br J Cancer* 84: 926–935, 2001.
53. **Oehrtman GT, Wiley HS, and Lauffenburger DA.** Escape of autocrine ligands into extracellular medium: experimental test of theoretical model predictions. *Biotechnol Bioeng* 57: 571–582, 1998.
54. **Peschon J, Slack J, Reddy P, Stocking K, Sunnarborg S, Lee D, Russell W, Castner B, Johnson R, Fitzner J, Boyce R, Nelson N, Kozlosky C, Wolfson M, Rauch C, Cerretti D, Paxton R, March C, and Black R.** An essential role for ectodomain shedding in mammalian development. *Science* 282: 1281–1284, 1998.
55. **Pierce K, Luttrell L, and Lefkowitz R.** New mechanisms in heptahelical receptor signaling to mitogen-activated protein kinase cascades. *Oncogene* 20: 1532–1539, 2001.

56. **Roovers K and Assoian R.** Integrating the MAP kinase signal into the G₁ phase cell cycle machinery. *Bioessays* 22: 818–826, 2000.
57. **Schlessinger J.** Cell signaling by receptor tyrosine kinases. *Cell* 103: 211–225, 2000.
58. **Schmidt-Ullrich R, Contessa J, Dent P, Mikkelsen R, Valerie K, Reardon D, Bowers G, and Lin P.** Molecular mechanisms of radiation-induced accelerated repopulation. *Radiat Oncol Investig* 7: 321–330, 1999.
59. **Schmidt-Ullrich RK, Dent P, Grant S, Mikkelsen RB, and Valerie K.** Signal transduction and cellular radiation responses. *Radiat Res* 153: 245–257, 2000.
60. **Sherrill J and Kyte J.** Activation of epidermal growth factor receptor by epidermal growth factor. *Biochemistry* 35: 5705–5718, 1996.
61. **Shoup D and Szabo A.** Role of diffusion in ligand binding to macromolecules and cell-bound receptors. *Biophys J* 40: 33–39, 1982.
62. **Shvartsman SY, Wiley HS, Deen WM, and Lauffenburger DA.** Spatial range of autocrine loops: modeling and computational analysis. *Biophys J* 81: 1854–1867, 2001.
63. **Simon M.** Receptor tyrosine kinases: specific outcomes from general signals. *Cell* 103: 13–15, 2000.
64. **Sporn M and Roberts A.** Autocrine secretion—10 years later. *Ann Intern Med* 117: 408–414, 1992.
65. **Swindle C, Tran K, Johnson T, Banerjee P, Mayes A, Griffith L, and Wells A.** Epidermal growth factor (EGF)-like repeats of human tenascin-C as ligands for EGF receptor. *J Cell Biol* 154: 459–468, 2001.
66. **Tan P and Kim S.** Signaling specificity: the RTK/RAS/MAP kinase pathway in metazoans. *Trends Genet* 15: 145–149, 1999.
67. **Waterman H and Yarden Y.** Molecular mechanisms underlying endocytosis and sorting of ErbB receptor tyrosine kinases. *FEBS Lett* 275: 142–152, 2001.
68. **Weiss GH.** *Aspects and Applications of the Random Walk.* Amsterdam: North-Holland, 1994.
69. **Wells A.** EGF receptor. *Int J Biochem Cell Biol* 31: 637–643, 1999.
70. **Werb Z and Yan YB.** Cell biology—a cellular striptease act. *Science* 282: 1279–1280, 1998.
71. **Wiley H and Burke P.** Regulation of receptor tyrosine kinase signaling by endocytic trafficking. *Traffic* 2: 13–18, 2001.
72. **Wiley HS, Woolf MF, Opresko LK, Burke PM, Will B, Morgan JR, and Lauffenburger DA.** Removal of the membrane-anchoring domain of epidermal growth factor leads to intracrine signaling and disruption of mammary epithelial cell organization. *J Cell Biol* 143: 1317–1328, 1998.
73. **Yarden Y and Sliwkowski M.** Untangling the ErbB signalling network. *Nat Rev Mol Cell Biol* 2: 127–137, 2001.
74. **Zhang Z, Oliver P, Lancaster JR Jr, Schwarzenberger PO, Joshi MS, Cork J, and Kolls JK.** Reactive oxygen species mediate tumor necrosis factor- α -converting, enzyme-dependent ectodomain shedding induced by phorbol myristate acetate. *FASEB J* 15: 303–305, 2001.
75. **Zwick E, Hackel P, Prenzel N, and Ullrich A.** The EGF receptor as central transducer of heterologous signalling systems. *Trends Pharmacol Sci* 20: 408–412, 1999.

